Kevin Lauer, Christian Möller, Dirk Schulze, Carsten Ahrens

Identification of photoluminescence P line in indium doped silicon as In_{Si}-Si_i defect

Original published in:
AIP Advances. - New York, NY : American Inst. of Physics. - 5 (2015), art. 017101, p. 1-11.
DOI: 10.1063/1.4905066
URL: http://dx.doi.org/10.1063/1.4905066
[Visited: 2015-01-16]

Identification of photoluminescence P line in indium doped silicon as In_{Si}-Si_i defect

Kevin Lauer,[1,a] Christian Möller,[1,b] Dirk Schulze,[2] and Carsten Ahrens[3]
[1]*CiS Forschungsinstitut für Mikrosensorik und Photovoltaik GmbH, Konrad-Zuse-Str. 14, 99099 Erfurt, Germany*
[2]*TU Ilmenau, Institut für Physik, Weimarer Str. 32, 98693 Ilmenau, Germany*
[3]*Infineon Technologies AG, Am Campeon 1-12, 85579 Neubiberg, Germany*

(Received 7 August 2014; accepted 15 December 2014; published online 7 January 2015)

Indium and carbon co-implanted silicon was investigated by low-temperature photoluminescence spectroscopy. A photoluminescence peak in indium doped silicon (P line) was found to depend on the position of a silicon interstitial rich region, the existence of a SiN_x:H/SiO_x stack and on characteristic illumination and annealing steps. These results led to the conclusion that silicon interstitials are involved in the defect and that hydrogen impacts the defect responsible for the P line. By applying an unique illumination and annealing cycle we were able to link the P line defect with a defect responsible for degradation of charge carrier lifetime in indium as well as boron doped silicon. We deduced a defect model consisting of one acceptor and one silicon interstitial atom denoted by A_{Si}-Si_i, which is able to explain the experimental data of the P line as well as the light-induced degradation in indium and boron doped silicon. Using this model we identified the defect responsible for the P line as In_{Si}-Si_i in neutral charge state and C_{2v} configuration. [http://dx.doi.org/10.1063/1.4905066]

I. INTRODUCTION

The shrinking size of structures in silicon microelectronic devices requires sharp dopant profiles. Due to the small atomic size and comparable high diffusivity of boron in silicon, boron cannot be processed with the required structure widths. Hence, there is a need to substitute boron by another acceptor species. One possible candidate is indium.[1] Indium exhibits a low diffusivity but the solubility as well as the electrically active fraction of indium in silicon is small. To control the indium dopant profile and the indium activation knowledge on the defects, which are formed by indium in silicon, is needed. The electrical activation of indium can be increased by co-doping with carbon[2] due to formation of indium-carbon pairs.[3] Further it is known that indium forms pairs with boron as well.[4] It was found by simulation that interstitial indium exists in a configuration with lowest formation energy where the indium atom is placed close to a substitutional position with a silicon interstitial nearby.[5] This defect is denoted by In_{Si}-Si_i. The known properties of indium related defects in silicon are not sufficient for a proper understanding of the indium activation in silicon.

A feature of indium doped silicon is the appearance of a peak in the low-temperature photoluminescence (PL) spectrum called P line.[6,7] Despite extensive research[8–17] the origin of the P line has not been identified yet. Experimentally, it was found that the P line is more pronounced in Czochralski than in float zone silicon.[7] The P line can be greatly enhanced by a short high temperature anneal with subsequent sharp quenching.[11] But this can be only achieved for samples treated in an oxygen containing atmosphere without a protective layer like SiN_x.[18] The intensity of the P line decreases

[a]klauer@cismst.de
[b]TU Ilmenau, Institut für Physik, Weimarer Str. 32, 98693 Ilmenau, Germany

due to isochronal annealing.[10] For silicon implanted with the radioactive isotope ^{111}In the P line was found to decrease much faster than expected from the half-life of the indium isotope.[19]

In this contribution we report on the impact of the position of a silicon interstitial rich region, a SiN_x:H/SiO_x stack at the surface and an illumination and annealing cycle on the P line in indium implanted silicon. The parameters of that cycle are taken from experiments on charge carrier lifetime changes in indium and boron doped silicon samples.[20] The results of this investigation imply that the defect, which is the origin of the P line and causes the changes in the carrier lifetime in boron and indium doped silicon, has the same structure in all cases. A detailed defect model based on an acceptor-silicon interstitial pair A_{Si}-Si_i is proposed. This defect model can be applied to explain the light-induced degradation observed in boron and indium doped silicon, too.

II. EXPERIMENTAL

Samples were fabricated from float zone silicon wafers (denoted by A to G) with a radius $r = 100$ mm, a thickness $t = 750$ μm and a boron base doping $[B_s] = (3\pm1) \times 10^{13}$ cm^{-3}. The latter value was determined using low-temperature PL spectroscopy.[21] The concentration of interstitial oxygen,[22] substitutional carbon[23] and interstitial nitrogen pairs[24] in the silicon wafers was measured by low-temperature FTIR spectroscopy to $[O_i] = 4 \times 10^{14}$ cm^{-3}, $[C_s] < 7 \times 10^{14}$ cm^{-3} and $[N_{2i}] = 3 \times 10^{14}$ cm^{-3}, respectively.

The wafers were implanted with indium and carbon. An overview of the used parameters for the implantations is given in Tab. I. The parameters of the carbon implantation were chosen in order to investigate the interaction of indium and carbon as well as the interaction of indium and silicon interstitials. The high energy carbon implant yields the projected range of the carbon peak at the same position as the peak of the indium concentration. Hence, the interaction of carbon and indium can be investigated in that case. The low energy carbon implant on the other hand yields a projected range of the carbon peak at half of the range of the indium peak. As a consequence silicon interstitials are put onto the indium peak.

The mechanism behind this approach is visualized in Fig. 1. The implantations for wafers F and G (see Tab. I) are simulated using TRIM.[25] Fig. 1 shows the simulated indium concentration profile as well as the silicon recoil atom concentration profile generated by the different carbon implantations. Amorphization of silicon due to implantation occurs if the silicon recoil concentration exceeds a threshold of $[Si_{recoil}] = 1.15 \times 10^{22}$ cm^{-3} (solid line in Fig. 1).[26] The amorphous/crystalline (a/c) interfaces for each carbon implantation are marked by dashed lines in Fig. 1. In the region of the amorphous layer above the a/c interface a low defect density can be achieved after solid phase epitaxial re-growth.[27] Beneath the a/c interface the implanted atoms generate an excess of silicon interstitial atoms (+1 *model*).[28] The existence of a silicon interstitial rich (SIR) region beneath the a/c interface is also evident due to the formation of so-called end-of-range (EOR) defects.[27,29] In the present investigation the formation of EOR defects is prevented by choosing proper annealing conditions. By engineering the position of the a/c interface using appropriate carbon implantation

TABLE I. Parameters of indium and carbon implantation. The radius of the measurement position is given as well.

wafer	implantation				sample	
	indium		carbon		1	2
	dose (cm^{-2})	energy (keV)	dose (cm^{-2})	energy (keV)	radius (mm)	
A	-	-	-	-	79	-
B	1.6×10^{12}	150	-	-	73	-
C	1.6×10^{12}	150	5.0×10^{14}	10	91	93
D	1.6×10^{12}	150	5.0×10^{14}	20	75	97
E	8.0×10^{11}	150	-	-	85	-
F	8.0×10^{11}	150	5.0×10^{14}	10	50	93
G	8.0×10^{11}	150	5.0×10^{14}	20	74	93

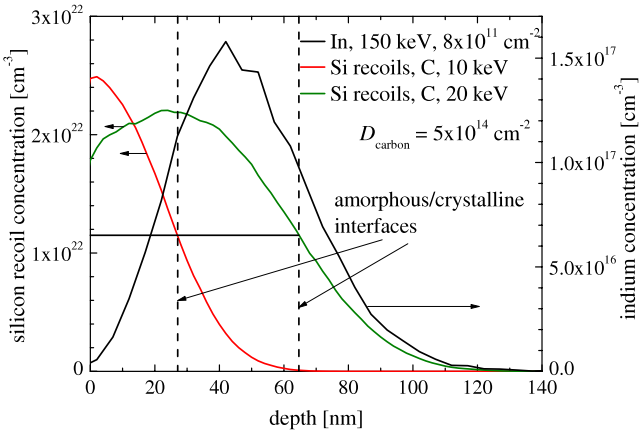

FIG. 1. Simulated concentration profiles of indium and recoiled silicon atoms for both carbon implantation energies (wafer F and G in Tab. I) as a function of depth. The amorphous/crystalline interfaces for each carbon implantation are marked by dashed lines.

parameters the SIR region can be placed onto the indium peak (wafer F) or behind the indium peak (wafer G) (see Fig. 1). Hence, in these samples the interaction of indium with silicon interstitials can be analyzed.

After implantation all wafers were identically processed. The implant was buried below a 400nm thick PECVD oxide layer. Three subsequent annealing steps were applied. First, the wafers got a rapid thermal process (RTP) at 1100 °C for 80 s followed by 600 °C for 10 s. Second, a furnace anneal at 1050 °C for 120 min was made followed by a cool down to 400 °C with a cooling rate of 5 °C/min. After that the samples were moved out of the furnace. The last step was an RTP oxidation at 1045 °C for 37 s followed by 600 °C for 7 s. Finally, the oxide layer was etched off and a protective layer consisting of SiN_x:H and SiO_x stack was deposited. This state of the wafers is denoted as untreated since no intentional illumination or low temperature annealing were done.

To measure PL spectra parts of the wafers were broken into samples of $\approx 15 \times 15$ mm^2. The samples were taken from the near edge region of the wafers with a radius $r > 50$ mm (see Tab. I). In the case of the samples without the protective SiN_x:H/SiO_x stack the layer was etched off by dipping the sample in a 5% HF solution for several minutes. Samples with and without the protective SiN_x:H/SiO_x stack are denoted by A_1 to G_1 and A_2 to G_2, respectively.

The low-temperature PL setup consists of a frequency doubled Nd:YAG Laser, a He flow cryostat, a double stage imaging monochromator with 2×750 mm focal length and two ruled gratings with 1200 grooves/mm, and a single InGaAs detector with conventional lock-in technique. PL spectra are taken using a laser power of 500 mW and a beam diameter of 2 mm. The spectra are measured while storing the samples in a bath of liquid helium.

Samples were illuminated and annealed following an unique cycle, which is usually applied to investigate light-induced degradation in boron and indium doped silicon.[20,30,31] To anneal the samples at 200 °C for 10 min a temperature controlled hotplate was used. The samples are illuminated by a halogen lamp with an intensity of about 0.1 Wcm^{-2}. While illumination the samples were stored on an aluminum plate to maintain a sample temperature of about 30 °C.

III. RESULTS AND DISCUSSION

In Fig. 2 PL spectra of sample F_2 are exemplarily shown for several steps of the illumination and annealing cycles. To allow a comparison of peak heights the PL intensity is normalised to yield the same peak height of the free exciton peak in each spectrum. PL peaks of excitons bound to the substitutional acceptors indium and boron (In_{NP}(BE), B_{TA}(BE) and B_{TO}(BE)) as well as the free exciton (I_{TO}(FE)) are clearly visible. As can be seen in Fig. 2 the applied illumination and annealing treatment has no impact on these PL lines. Two further lines called P and R[7] appear in the spectra.

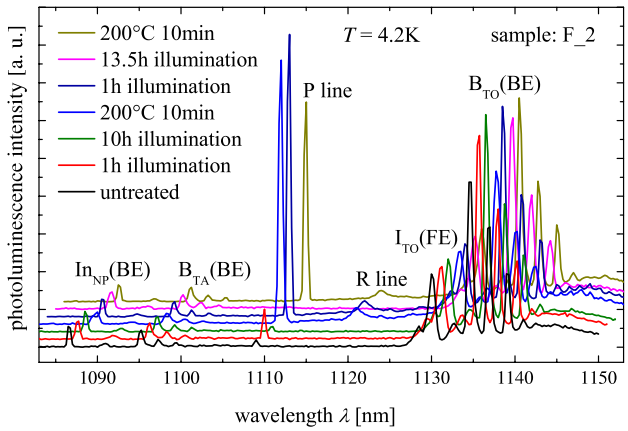

FIG. 2. PL spectra of sample F_2 after different steps of the illumination and annealing cycle. The spectra are shifted in x and y direction for clarity. The spectra are normalised with respect to the peak height of the free exciton I_{TO}(FE) peak.

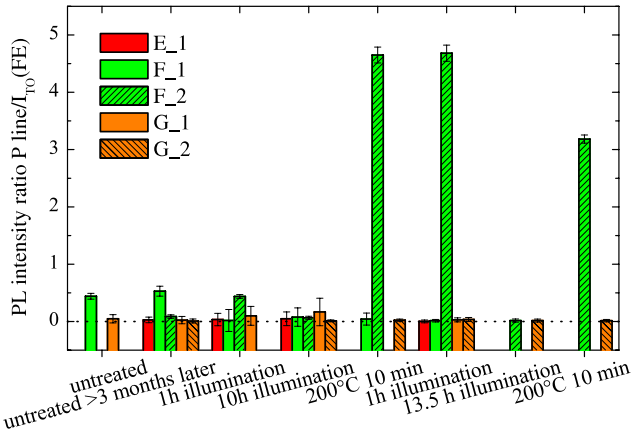

FIG. 3. PL intensity ratio of P line and free exciton during the illumination and annealing treatment for samples implanted with the low indium dose. In the case of missing bars the samples were annealed or illuminated but no measurement was done.

These lines are significantly affected by the specific illumination and annealing treatment. In the following the PL ratio of the P line peak height and the peak height of the free exciton are evaluated.

In Fig. 3 the PL intensity ratio of P line and free exciton is depicted during the illumination and annealing treatment for samples implanted with the low indium dose. Error bars were obtained from the noise of the spectra. In the case of missing bars the samples were annealed or illuminated but no measurement was done. From Fig. 3 it is found that the intensity of the P line is influenced by three factors, which are the position of a SIR region, the existence of a SiN_x:H/SiO_x stack at the surface and the illumination and annealing cycle. These will be discussed separately in the following.

A. Variation of SIR region

As discussed in section II samples are prepared in a way that a SIR region is placed onto the indium peak or behind the indium peak by using appropriate parameters of the carbon co-implantation. This implantation regime enables the discussion of the experimental results in frame of a direct participation of silicon interstitial atoms. The annealing steps, which are applied after the implantation, do not alter this main statement of the experiment.

The first RTP step leads to a re-crystallization of the amorphous layer and to an annealing of the implantation damage beneath the a/c interface. During subsequent cool down silicon interstitials in the SIR region are captured by substitutional indium atoms, substitutional carbon atoms or

complexes containig several carbon atoms.[32] Indium has some advantage in this competition due to its negative charge state leading to a larger capture cross section for positively charged silicon interstitials.[33] A clear difference in the amount of indium atoms which have captured a silicon interstitial is expected if the implantation regimes depicted in Fig. 1 are compared. In case where the indium peak is located mainly above the a/c interface (wafer G) indium can not capture any silicon interstitial atoms because there are no excess silicon interstitial atoms after re-crystallization of the amorphous layer.[27] After the indium atom has captured a silicon interstitial atom it will form the In_{Si}-Si_i defect since this is the configuration with the lowest formation energy.[5]

It is known that a short high temperature anneal with subsequent fast quenching of the sample,[11] e.g. by dropping it into water, generates the P line. Since, in the present experiment two RTP steps are applied the generation of the P line due to these steps has to be prevented. This was done by a short 600 °C annealing step following both RTP steps. Fast cooling from 600 °C was found to not generate the P line.[16]

The second prolonged annealing step (see section II) leads to a diffusion of carbon, oxygen and indium into the silicon bulk region. Oxygen originates from the silicon oxide layer at the surface. Since, carbon and oxygen have a higher diffusivity compared to indium[34] they will establish a constant background concentration at their respective solubility limits in the region of the indium peak. The solubility limits at 1045 °C are about 10^{16} cm^{-3} for carbon and 1.4×10^{17} cm^{-3} for oxygen.[34] In case of indium it is known that it is preferably difussing via an interstitialcy mechanisms.[5,35,36] mediated by the In_{Si}-Si_i defect.[5] Since, the In_{Si}-Si_i defect is the main diffusing species the difference in the In_{Si}-Si_i defect density, which was generated by varying the SIR region in the samples, remains during indium diffusion.

One could argue that the implanted carbon atoms impact the indium diffusion in a way that substitutional carbon consumes the silicon interstitial atoms. Indeed a suppression of the indium diffusion by an epitaxial grown carbon rich layer was observed.[37] Since, the amorphous layer is re-crystallized in the first annealing step of our experiment carbon resides on substitutional places above the a/c interface (see Fig. 1). A consumption of silicon interstitial atoms by substitutional carbon during the second annealing step could be expected. But this would even enhance the difference in silicon interstitial atom content between the present two carbon co-implantations. In case of a carbon implantation below the amorphisation threshold an enhancement or retardation of silicon interstitial mediated diffusion is a controversial issue.[38] It was observed in case of boron, which also diffuses via the B_{Si}-Si_i defect,[39] that implanted carbon enhances the diffusion at 1000 °C.[38] The third short annealing step leads to a further diffusion of the three species.

The discussion of the present experimental data with respect to a defect composed of an indium and a silicon interstitial atom is simplified due to the extensive research on the P line which has been done in the past. From these experiments it is clear that the two species appearing in the present investigation carbon and oxygen can be ruled out as components of the defect. Oxygen was found to have an impact but not in a way that it is directly involved in the defect responsible for the P line.[18] The differences observed for the P line in the different wafers of the present experiment can not be explained by the oxygen content since the indiffused oxygen content is the same for all investigated wafers. In case of carbon a correlation of the P line to the carbon concentration in the samples has never been found.[8–11] The appearance of the P line in indium implanted state-of-the-art Czochralski silicon without any carbon co-implantation[16,17] rule out the incorporation of carbon in that defect as well. The most simple defect consisting of an indium and a carbon atom In_s-C_s is known as an acceptor.[3] We found the characteristic absorption peak of In_s-C_s in our low temperature FTIR experiments. But from present literature a correlation of the P line and the In_s-C_s can be clearly ruled out.

In case of the reference sample E_1, which does not possess a carbon co-implantation at all, the P line does not appear in all measured PL spectra as shown in Fig. 3. The same holds for the samples G_1 and G_2, where the SIR region is placed beneath the indium peak. In contrast to that the samples F_1 and F_2 show a pronounced intensity of the P line at several illumination and annealing steps. The most striking results are obtained after both annealing steps. In these cases a strong increase in the P line intensity is visible for sample F_2, whereas sample G_2 does not increase. Since, the only difference between sample F_2 and G_2 is the position of the SIR region

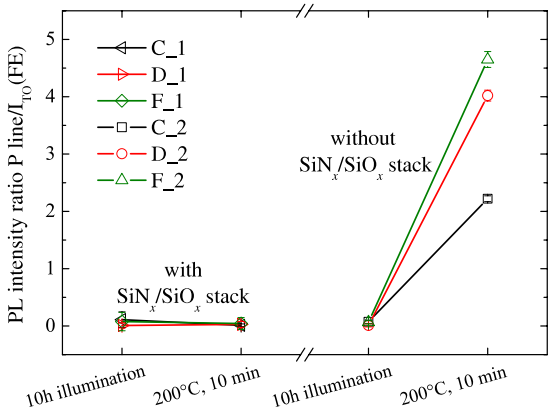

FIG. 4. P line intensity ratio after illumination and annealing with and without protective SiN_x:H/SiO_x stack on the surface of the samples.

we conclude that in sample F_2 silicon interstitials, which are put onto the indium peak (see Fig. 1), are involved in the defect responsible for the P line.

The comparison of different carbon implantations was not possible in the case of samples with the high indium dose (B, C and D) for two reasons. First, the P line appears in all investigated samples. This may be caused by the higher density of silicon interstitials generated by the indium implantation itself. The second reason is that samples C_2 and D_2 are not directly comparable as the position in the wafer differs. It seems that the P line increases with increasing radius of the measurement position. This can be explained by an increase of the density of silicon interstitials near the edge of the silicon crystal.

B. SiN_x:H/SiO_x stack

We found that a protective SiN_x:H/SiO_x stack on the surface of the samples impacts the PL intensity of the P line. With that stack on the surface the P line does not appear after the 10 min and 200 °C annealing step in all investigated samples. For the samples, which exhibit the largest P line intensity, the impact of the stack at the surface is depicted in Fig. 4. Since SiN_x:H layers contain hydrogen in reasonable amounts we conclude that hydrogen influences the defect, which causes the P line. During the annealing step hydrogen is able to diffuse into the near surface region of the silicon. Since the implantation depth is in the order of 100 nm hydrogen is able to interact with the defect responsible for P line. A similar behaviour was recently found in the B_{Si}-Si_i case. The permanent deactivation for that defect is only possible if hydrogen is available in the silicon.[40]

C. Illumination and annealing cycle

Since the PL measurements of the untreated samples (see Fig. 2) show a clear sign that silicon interstitials are involved in the defect responsible for the P line we suspected the defect to be the In_{Si}-Si_i defect as proposed in Ref. 20. Hence, we applied the unique illumination and annealing cycle for the A_{Si}-Si_i defect.[20,30,31] We found after etching off the protective SiN_x:H/SiO_x stack at the surface of the samples that the P line is indeed following that cycle. The results of these measurements are depicted in Fig. 5. A prolonged illumination treatment of at least 10 h at an intensity of 0.1 Wcm^{-2} and a temperature of about 30 °C leads to a complete disappearance of the P line. After the annealing step of 200 °C for 10 min the P line appeared again. As expected this process is reversible. Interestingly, the P line increases further after 1 h illumination. It is known from lifetime measurements[20] that the degradation takes place in two steps with different time constants, respectively. Hence, we conclude that the defect responsible for the P line corresponds to the intermediate state of the lifetime degrading defect. By applying the defect model proposed in section IV this intermediate state is identified with $(In_{Si}\text{-}Si_i)^0$ in C_{2v} configuration.

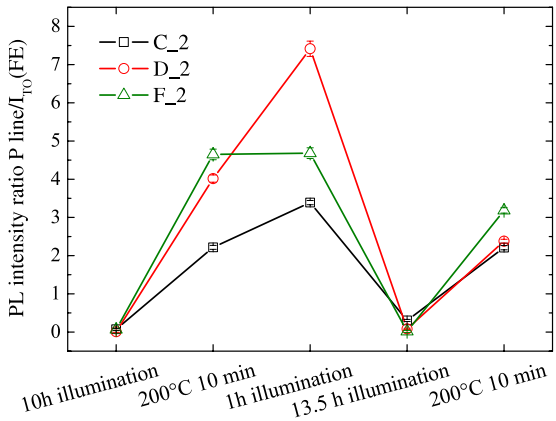

FIG. 5. Change of the P line intensity ratio during illumination and annealing cycles.

IV. A_{Si}-Si$_i$ DEFECT

A. Model

The A_{Si}-Si$_i$ defect model is visualized in Fig. 6 and 7. Fig. 6 depicts the atomic structure of the A_{Si}-Si$_i$ defect for the case of boron in two possible configurations C_{3v} and C_{1h} as found by simulation.[41] In Fig. 7(a) a schematic diagram of total energy curves as function of configuration coordinates for charge states (+), (0) and (-) of the A_{Si}-Si$_i$ defect is shown for the case of *p*-type silicon. Stable atomic configurations are denoted by S_1 and S_2. The model is mainly deduced from simulation results of the B_{Si}-Si$_i$ defect.[41] where S_1 and S_2 equals C_{3v} and C_{1h}, respectively. In case of indium the exact atomic configurations for each charge state are not as clear. The defect responsible for the P line was found to have C_{2v} symmetry.[10,15,42] Simulation results indicate C_{1h} for the In_{Si}-Si$_i$ defect but without information on the charge state.[5] Hence, we tentatively identify the atomic configurations S_1 and S_2 in case of indium to have C_{2v} and C_{1h} symmetry, respectively. Possible states of the A_{Si}-Si$_i$ defect are denoted by numbers 1 to 5 in circles. Fig. 7(b) summarizes literature data on electronic levels within the band gap of the B_{Si}-Si$_i$ defect. Basically, the A_{Si}-Si$_i$ defect exists in two different atomic configuration denoted by S_1 and S_2. For each atomic configuration several charge states are possible.

The unique cycle, which was applied in the experiments, changes the charge state as well as the atomic configuration of the A_{Si}-Si$_i$ as follows: The state of the A_{Si}-Si$_i$ defect with lowest total energy is $(A_{Si}\text{-Si}_i)^+$ in S_1 configuration denoted by 1 in Fig. 7(a). This is the state formed after 10 min annealing step at 200 °C. By illumination, which causes generation of charge carriers, the A_{Si}-Si$_i$ defect traps an electron with a characteristic time constant and becomes neutral (denoted

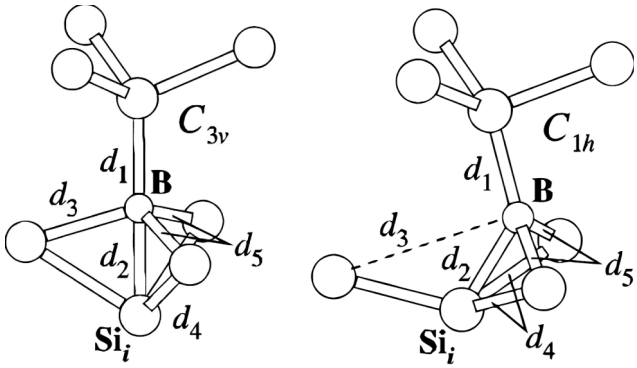

FIG. 6. Atomic structure of the A_{Si}-Si$_i$ defect for the case of boron in the two possible configuration C_{3v} and C_{1h}. (after Ref. 41)

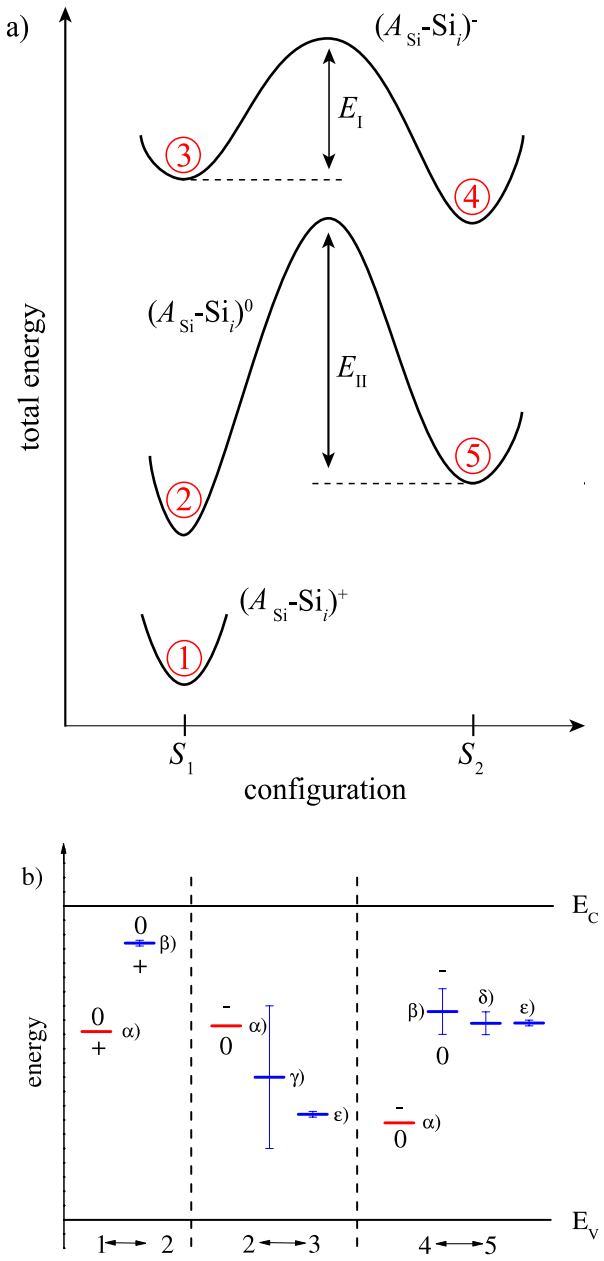

FIG. 7. a) Schematic diagram of total energy curves as function of configuration coordinates for charge states (+), (0) and (-) of the A_{Si}-Si_i defect in *p*-type silicon. b) Energy diagram of the electronic levels within the bandgap of silicon in the case of the B_{Si}-Si_i defect. Simulation and measurement data are colored red and blue, respectively. Refs. α) 41, β) 43, γ) 31, δ) 44, ϵ) 45.

by 2). State 2 in Fig. 7(a) is the intermediate state which is found after about 1 h illumination at 30 °C. If the illumination is stopped at that point the $(A_{Si}\text{-}Si_i)^0$ will emit the electron (step 2 to 1) with a characteristic time constant and the ground state 1 is reached again. The transition rate for process 2 to 1 in case of boron is depicted in Fig. 8.

While further illumination the neutral $(A_{Si}\text{-}Si_i)^0$ defect will capture an electron (step 2 to 3) and hence will be negatively charged. In the negatively charged state the S_2 atomic configuration is energetically favoured[41] and hence an atomic reconfiguration from S_1 to S_2 will take place (step 3 to 4). The energy barrier E_I for the reconfiguration will be low since the process takes place at room temperature. Since, the characteristic time constant of this process is in the range of 10^3 s at

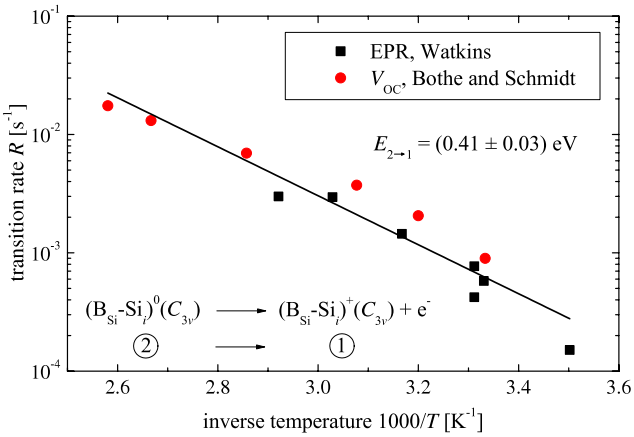

FIG. 8. Arrhenius plot of the transition rate of the A_{Si}-Si_i defect in case of boron from state 2 to 1 in Fig. 7(a). Data are taken from Refs. 48 and 31

room temperature the reconfiguration has nearly completed after 10 h. After turning off illumination the $(A_{Si}\text{-}Si_i)^-$ in S_2 configuration will emit an electron and becomes neutral (step 4 to 5). The S_2 configuration in the positive charge state was not found by the simulations.[41] The energy barrier E_{II} for the change of the configuration from S_2 to S_1 in neutral charge state must be higher since the configuration change (step 5 to 2) will take place only at elevated temperatures (200 °C for 10 min). Hence, $(A_{Si}\text{-}Si_i)^0$ in S_2 configuration (state 5) is stable at room temperature.

In case of charge carrier lifetime measurements in boron[30,31,46,47] and indium[20] doped silicon process 1 to 2 is identified with the fast component of charge carrier lifetime degradation. The transition from state 1 to 2 enables the recombination of electron hole pairs via the second deeper lying level (see Fig. 7(b)) and hence causes the observed fast degradation in carrier lifetime. The reconfiguration of the atomic structure (process 3 to 4) is indentified with the slow component visible in carrier lifetime measurements. In S_2 configuration a new electronic level is introduced (see Fig. 7(b)) which cause the observed further degradation of carrier lifetime.

In case of PL measurements all changes in charge state as well as atomic configuration of the A_{Si}-Si_i defect will take place as described above, but the PL peaks can be only attributed to one specific state. In section III C the P line is found to correspond to the intermediate state, which is set up after a 200 °C annealing step for 10 min followed by 1 h illumination. By applying the model we are now able to identify the P line with the A_{Si}-Si_i defect in neutral charge state and S_1 configuration which is in case of indium $(In_{Si}\text{-}Si_i)^0$ in C_{2v} configuration.

B. Discussion of experimental data

Experimentally, the parameters of the A_{Si}-Si_i defect kinetic in case of boron were thoroughly investigated.[31] The energy barriers were determined to E_I = (0.475 ± 0.035) eV and E_{II} = (1.32 ± 0.05) eV. Interestingly, the transition rate of the B_{Si}-Si_i in C_{3v} configuration from neutral to positive charge state (step 2 to 1) was observed by the disappearance of the Si-G28 spectrum in EPR measurements[48] as well as by open circuit voltage V_{OC} measurements of solar cells.[31,49] These data are reassembled in Fig. 8. The good agreement of these data support the thesis that the boron interstitial B_i, which was investigated by EPR[48] and later identified as the B_{Si}-Si_i defect,[41,50] is identical with the defect responsible for at least the fast component of the light-induced degradation in boron doped silicon.[31] In frame of the A_{Si}-Si_i defect model it is possible to explain consistently the observed phonemena of the light-induced degradation in boron doped silicon like the fast and slow component, the impact of illumination and annealing steps and the reversibility by electron capture and emission as well as by rearrangement of atomic configurations.

In contrast to boron the density of experimental data in case of indium is smaller. But the known data support our model and conclusion that the P line is caused by excitons bound to

$(In_{Si}\text{-}Si_i)^0$ in C_{2v} configuration. The P line is found to disappear by isothermal annealing[10] in darkness.[51] This is interpreted similar to the boron case as the transition from 2 to 1 in Fig. 7(a). It is observed that the P line disappears after prolonged storing samples at room temperature,[16,17] too. In this experiment the samples were store in transparent plastic boxes in the laboratory.[52] Hence, it is possible that in this experiment the daylight induces the transition of the $In_{Si}\text{-}Si_i$ defect into the neutral state in C_{1h} configuration (steps 2 to 5), which yields the disappearance of the P line. Another experiment investigates the P line in silicon implanted with the radioactive isotope ^{111}In.[19] The P line was found to disappear much faster than the exciton bound to substitutional indium. In frame of our model this finding can be interpreted as follows: The γ quanta emitted by the radioactive decay of ^{111}In generate charge carriers in the silicon which induce the transition into the negative or neutral state in C_{1h} configuration. It was found that a short high temperature anneal with a very fast quenching of the samples increases the P line significantly.[11] Possibly, $In_{Si}\text{-}Si_i$ defects are formed in the bulk or only at the surface.[53,54] by this treatment due to increased equilibrium concentration of silicon interstitials at high temperatures.[34] The fast quench is needed to prevent the recombination of interstitials with vacancies.[34]

Following the model depicted in Fig. 6 and Fig. 7 the P line in Figs. 2-5 should only be visible after 1h illumination with the annealing step before. This is not seen. As known from the boron case,[31,48] by illumination the $A_{Si}\text{-}Si_i$ defect will approach state 2 even at liquid helium temperature quite fast. Unfortunately we did not account for that effect in our experiments yet. During justification of the samples and during recording the spectra at wavelengths below the P line position the samples are illuminated with intense laser light for several minutes. Hence, some $(In_{Si}\text{-}Si_i)^0$ in C_{2v} configuration will have formed in the PL measurement directly after the annealing step.

The $A_{Si}\text{-}Si_i$ defect model is in this contribution only discussed for the cases boron and indium but there are hints that the model will be applicable for thallium as well. In thallium doped silicon photoluminescence peaks are found, which have remarkable similarities to the P line in indium doped silicon.[14,55] This points to the existence of a $Tl_{Si}\text{-}Si_i$ defect. In fact in case of thallium two groups of lines exists which undergo a transition under illumination.[14] This transition can be identified with process 1 to 2 in Fig. 7(a).

V. CONCLUSION

In conclusion we investigated indium and carbon co-implanted silicon by PL spectroscopy. A characteristic PL peak in indium doped silicon denoted by P line was observed. We found that the intensity of the P line is influenced by three factors, which were the position of a silicon interstitial rich region, the existence of a SiN_x:H/SiO_x stack at the surface and an illumination and annealing cycle. By interpreting the dependence of the P line intensity on the position of a silicon interstitial rich region we concluded that silicon interstitials are involved in the defect responsible for the P line. Since a SiN_x:H/SiO_x stack at the surface prevents the appearance of the P line we concluded that hydrogen impacts the defect configurations. By applying a unique illumination and annealing cycle we were able to relate the changes of the P line to changes in the charge carrier lifetime in indium as well as boron doped silicon. Due to this established relation we were able to deduce a detailed model for a defect consisting of an acceptor and a silicon interstitial atom denoted by $A_{Si}\text{-}Si_i$. It was shown that this defect model is able to explain the observed properties. By applying that model to the PL measurements of the P line we identified the $In_{Si}\text{-}Si_i$ in neutral charge state and C_{2v} configuration as the defect, which is the cause for the P line. It was also found that the $A_{Si}\text{-}Si_i$ defect model is able to explain the light-induced degradation in boron and indium doped silicon.

ACKNOWLEDGMENTS

The authors thank J. Weber, M. Tajima, K. Terashima, J. Vanhellemont and M. Hakala for fruitful discussions. K. Bothe is acknowledged for providing the data points in Fig. 8. This work was partially funded by Bundesministerium für Wirtschaft und Technologie under contract number

VF120025. We acknowledge support for the Article Processing Charge by the German Research Foundation and the Open Access Publication Fund of the Technische Universität Ilmenau.

[1] S. Biesemans, S. Kubicek, and K. D. Meyer, Japanese Journal of Applied Physics **35**, 1037 (1996).
[2] H. Boudinov, J. P. d. Souza, and C. K. Saul, Journal of Applied Physics **86**, 5909 (1999).
[3] C. E. Jones, D. Schafer, W. Scott, and R. J. Hager, Journal of Applied Physics **52**, 5148 (1981).
[4] S. Scalese, S. Grasso, M. Italia, V. Privitera, J. S. Christensen, and B. G. Svensson, Journal of Applied Physics **99**, 113516 (2006).
[5] P. Alippi, A. La Magna, S. Scalese, and V. Privitera, Physical Review B **69**, 085213 (2004).
[6] M. A. Vouk and E. C. Lightowlers, Journal of Luminescence **15**, 357384 (1977).
[7] G. S. Mitchard, S. A. Lyon, K. R. Elliott, and T. C. McGill, Solid State Communications **29**, 425 (1979).
[8] U. O. Ziemelis, R. R. Parsons, and M. Voos, Solid State Communications **32**, 445 (1979).
[9] D. H. Brown and S. R. Smith, Journal of Luminescence **21**, 329 (1980).
[10] J. Weber, R. Sauer, and P. Wagner, Journal of Luminescence **2425, Part 1**, 155 (1981).
[11] M. L. W. Thewalt, U. O. Ziemelis, and P. R. Parsons, Solid State Communications **39**, 27 (1981).
[12] J. Wagner and R. Sauer, Physical Review B **27**, 6568 (1983).
[13] S. P. Watkins, M. L. W. Thewalt, and T. Steiner, Solid State Communications **46**, 447 (1983).
[14] S. P. Watkins, M. L. W. Thewalt, and T. Steiner, Physical Review B **29**, 5727 (1984).
[15] S. P. Watkins and M. L. W. Thewalt, Physical Review B **34**, 2598 (1986).
[16] K. Terashima and T. Matsuda, Japanese Journal of Applied Physics **41**, 1203 (2002).
[17] K. Terashima and M. Horikawa, Physica B: Condensed Matter **401402**, 134 (2007).
[18] T. Brown and P. Bradfield, Physical Review B **37**, 2699 (1988).
[19] S. E. Daly, M. O. Henry, K. Freitag, and R. Vianden, Journal of Physics: Condensed Matter **6**, L643 (1994).
[20] C. Möller and K. Lauer, physica status solidi (RRL) - Rapid Research Letters **7**, 461 (2013).
[21] Semiconductor Equipment and Materials International, SEMI MF1389-0704 (2004).
[22] P. Wagner, Applied Physics A **53**, 2025 (1991).
[23] Semiconductor Equipment and Materials International, SEMI MF1391-1107 (2012).
[24] P. Wagner, R. Oeder, and W. Zulehner, Applied Physics A **46**, 7376 (1988).
[25] J. F. Ziegler, M. Ziegler, and J. Biersack, Nuclear Instruments and Methods in Physics Research Section B: Beam Interactions with Materials and Atoms **268**, 1818 (2010).
[26] H. Cerva and G. Hobler, Journal of The Electrochemical Society **139**, 3631 (1992).
[27] L. Pelaz, L. A. Marqus, and J. Barbolla, Journal of Applied Physics **96**, 5947 (2004).
[28] M. D. Giles, Journal of the Electrochemical Society **138**, 1160 (1991).
[29] G. Z. Pan, K. N. Tu, and A. Prussin, Journal of Applied Physics **81**, 78 (1997).
[30] H. Fischer and W. Pschunder, *Proceedings of the tenth IEEE Photovoltaic Specialists Conference* (1973), p. 404.
[31] K. Bothe and J. Schmidt, J. Appl. Phys. **99**, 013701 (2006).
[32] A. Mattoni, F. Bernardini, and L. Colombo, Physical Review B **66** (2002).
[33] A. R. Bean, S. R. Morrison, R. C. Newman, and R. S. Smith, Journal of Physics C: Solid State Physics **5**, 379 (1972).
[34] P. Pichler, *Intrinsic point defects, impurities, and their diffusion in silicon* (Springer, 2004).
[35] D. A. Antoniadis, Journal of Applied Physics **53**, 9214 (1982).
[36] S. Solmi, A. Parisini, M. Bersani, D. Giubertoni, V. Soncini, G. Carnevale, A. Benvenuti, and A. Marmiroli, Journal of Applied Physics **92**, 1361 (2002).
[37] C. F. Tan, E. F. Chor, J. Liu, H. Lee, E. Quek, and L. Chan, Applied Physics Letters **83**, 4169 (2003).
[38] M. Uematsu, Journal of Applied Physics **111**, 073517 (2012).
[39] S. Mirabella, D. De Salvador, E. Napolitani, E. Bruno, and F. Priolo, Journal of Applied Physics **113**, 031101 (2013).
[40] S. Wilking, A. Herguth, and G. Hahn, Journal of Applied Physics **113**, 194503 (2013).
[41] M. Hakala, M. J. Puska, and R. M. Nieminen, Physical Review B **61**, 8155 (2000).
[42] R. Sauer and J. Weber, Physica B+C **116**, 195 (1983).
[43] R. D. Harris, J. L. Newton, and G. D. Watkins, Physical Review B **36**, 1094 (1987).
[44] S. Rein and S. W. Glunz, Applied Physics Letters **82**, 1054 (2003).
[45] T. Mchedlidze and J. Weber, physica status solidi (RRL) Rapid Research Letters (2014).
[46] R. L. Crabb, Proceedings of the 9th IEEE Photovoltaic Specialists Conference 329 (1972).
[47] K. Graff and H. Pieper, Phys. Stat. Sol. (a) **30**, 593 (1975).
[48] G. D. Watkins, Physical Review B **12**, 5824 (1975).
[49] Stage two of the annihilation process of the fast component within their publication is in fact the annihilation process of the slow component., K. Bothe private communication.
[50] E. Tarnow, EPL (Europhysics Letters) **16**, 449 (1991).
[51] J. Weber, private communication.
[52] K. Terashima, private communication.
[53] L. I. Fedina and A. L. Aseev, Sov. Phys. Solid State **32**, 33 (1990).
[54] J. Vanhellemont, A. Romano-Rodriguez, L. Fedina, J. Van Landuyt, and A. Aseev, Materials Science and Technology **11**, 1194 (1995).
[55] M. L. W. Thewalt, U. O. Ziemelis, and R. R. Parsons, Physical Review B **24**, 3655 (1981).